Cloud top height comparisons from ASTER, MISR, and MODIS for trade wind cumuli

Iliana Genkova [a,*], Gabriela Seiz [b], Paquita Zuidema [c], Guangyu Zhao [a], Larry Di Girolamo [a]

[a] *Department of Atmospheric Sciences, University of Illinois at Urbana-Champaign, USA*
[b] *MeteoSwiss, Switzerland*
[c] *RSMAS, University of Miami, USA*

Abstract

ASTER stereo and ASTER infrared (IR) retrieved cloud top heights (CTHs) at 90 m spatial resolution are compared to operational Multi-Angle Imaging SpectroRadiometer (MISR) stereo and MODerate Resolution Imaging Spectroradiometer (MODIS) thermal IR techniques at 1100 m and 5000 m spatial resolution, respectively. ASTER data availability limits this study to trade wind cumulus clouds only. ASTER IR, MISR stereo and MODIS IR cloud height frequency distributions were derived for 41 trade wind cumulus cloud scenes with no cirrus contamination. All three retrievals produce a bimodal CTH distribution with maxima at 650 and 1500 m.

Several scenes are investigated in further details utilizing the ASTER stereo heights. The ASTER stereo-derived CTH frequency distribution is also bimodal and coincides best with a surface-based ceilometer-derived cloud base height distribution, in the sense that it produces the fewest CTH retrievals below the typical lidar-observed cloud base height. Sensitivity to spatial resolution was investigated by degrading ASTER stereo and IR CTH retrievals to the MISR spatial resolution, and also by deriving ASTER stereo heights from degraded radiances. The degraded ASTER stereo CTH retrievals remain bimodal, but showed less high clouds and more lower clouds, whereas the ASTER stereo heights from degraded radiances lose the bimodal structure similarly to the ASTER degraded resolution IR technique.

Overall, the stereo technique appears more suitable for retrieving CTH for trade wind cumulus clouds than IR techniques, because it shows less sensitivity to resolution. With either technique CTHs should be produced at the high spatial resolution (finer than 1 km) and with subsampling preferred over spatial averaging, if necessary. Nonetheless, even at a spatial resolution of 1 km (which often exceeds the horizontal size of many trade wind cumulus clouds) both stereo and IR techniques reflect the CTH bimodality characterizing the scenes we studied.
© 2006 Elsevier Inc. All rights reserved.

Keywords: Trade wind cumulus; Cloud top height; ASTER; MISR; MODIS

1. Introduction

Cumulus clouds are one of the most commonly occurring cloud types on Earth. They account for an average coverage of 12% over the ocean (Warren et al., 1986) and produce a significant amount of precipitation (Short & Nakamura, 2000) to impact Earth's water and energy cycles. Despite the importance of cumuli to global climate, their radiative and latent heating effects remain poorly depicted in current global climate models (e.g., Bony & Dufresne, 2005). Although there are many

properties of cumuli that are important to measure, we will focus on cloud top height, not only for its impact on radiation, but also for its link to rain production (e.g., Rangno & Hobbs, 2005). It has been both observed and modeled that the properties of cumuli, such as cloud top height and precipitation, can be modified by aerosols (e.g., McFarquhar et al., 2004; Xue & Feingold, 2006). Therefore, the need to measure cloud top height accurately over the globe is imperative for climate research.

For shallow cumuli, such as those observed over the trade wind region of Earth, measuring their cloud top altitude from space has been difficult. Trade wind cumulus cloud populations are typically dominated by clouds with horizontal sizes less than 1 km (Benner & Curry, 1998; Zhao & Di Girolamo, in press),

while the spatial resolutions of meteorological satellite instruments are on the order of a kilometer or more. This disparity means that a conventional cloud-top altitude remote sensing technique relying on infrared brightness temperatures will be sensitive to the cloud fractional coverage of a pixel, and, for optically-thin clouds, to the cloud infrared emissivity (e.g., Rossow & Garder, 1993). The focus of this paper is a preliminary comparison and examination of a suite of techniques for satellite retrievals of trade-wind cumulus cloud-top height, utilizing different instruments from the EOS Terra satellite platform. The region was selected to coincide with the Rain in Cumulus over the Ocean (RICO) experiment (http://www.joss.ucar.edu/rico), held from November 2004 to January 2005 in the Caribbean Sea near Antigua. A unique aspect of the paper is the inclusion of Advanced Spaceborne Thermal Emission and Reflection Radiometer (ASTER) data. Data from the ASTER instrument were requested and collected over 10–20 N, 55–65 W from September 2004 through March 2005. ASTER data are of interest because of their high native spatial resolution — 15 m to 90 m depending on wavelength. In situ data from RICO, ASTER IR and stereo techniques, the IR technique used by the MODerate Resolution Imaging Spectroradiometer (MODIS) standard product, and the stereo technique used by the Multi-Angle Imaging Spectroradiometer (MISR) standard product are examined to better understand the quality and limitation of cloud top height retrievals for trade wind cumuli. Section 2 describes the datasets, Section 3 provides the analysis and results, and Section 4 summarizes our findings.

2. Terra instruments and data sets

2.1. ASTER

ASTER is a high-resolution remote sensing imager primarily used for land surface studies. The ASTER instrument measures radiances in 14 channels over a 60-km-wide swath. The visible and near-infrared channels range from 0.5 μm to 0.9 μm and have 15 m resolution; the short-wave infrared channels with 30 m resolution are between 1.6 μm and 2.43 μm; and the thermal infrared (TIR) channels between 8 μm and 12 μm have 90 m resolution. There are two telescopes for the 0.76 to 0.86 μm band-one nadir and one looking backward at an angle of 26.7°, thus allowing stereo analysis. More details on the ASTER instrument and its performance can be found in Yamaguchi et al. (1998). Cloud properties are not operationally derived from the ASTER data. However, two retrieval algorithms have been developed and applied to derive trade wind cumulus CTHs from ASTER.

2.1.1. ASTER stereo heights

Stereo CTHs were derived from the ASTER 0.8 μm nadir/backward stereo pair at 15 m resolution, using the methodology described by Seiz et al. (2002). Matching was constructed for each cloudy pixel using the ASTER 15-m cloud mask derived in Zhao and Di Girolamo (in press), providing a very dense CTH grid. The preliminary CTHs were subsequently corrected for the height error introduced by cloud motion during the time delay

between acquisition of the nadir and backward views. In contrast to MISR, winds cannot be retrieved from the ASTER data itself, and instead cloud-tracked winds are extracted from Geostationary Operational Environmental Satellite (GOES) (Velden et al., 2005). GOES-derived winds' errors introduce the largest uncertainty in ASTER stereo CTH retrievals (Seiz et al., 2006).

2.1.2. ASTER infrared heights

ASTER 12 μm data (channel 14) were used to retrieve the cloud height for each 90 m cloudy pixel. This wavelength experiences the least amount of water vapor absorption among the ASTER TIR channels. Details of the algorithm to retrieve CTH from channel 14 of ASTER are given in Zhao and Di Girolamo (in press). In brief, a 90 m pixel is flagged as cloudy only if *all* the 15 m subpixels within the corresponding 0.8 μm nadir scene are considered cloudy based on the 15 m cloud mask, this ensures fully cloud 90-m pixels and increases the probability that the emissivity of the cloud is closer to one. The thermal radiance for each 90 m cloudy pixel is converted into a brightness temperature (BT) following Alley and Jentoft-Nilsen (2001). Finally, the BT is converted into a CTH using the nearest-in-time sounding temperature profiles from the island of Guadeloupe. Only soundings from Guadeloupe were utilized, as these provided a longer, more temporally regular time series than those from the RICO experiment. The uncertainty in CTH for the clouds observed by the ASTER channel 14 technique were conservatively placed at ∼400 m (Zhao & Di Girolamo, in press).

2.2. MISR

MISR has four spectral bands centered at 446 nm, 558 nm, 672 nm, and 866 nm. It views the earth with its nine push-broom cameras-four forward, one nadir, and four backward looking. Relative to the earth surface, the viewing angles are 0°±26.1°, ±45.6°, ±60.0°, and ±70.5°. The time interval for a scene to be viewed by all cameras is 7 min, and the swath width is about 400 km. The spatial resolution ranges from 275 m to 1100 m, depending on spectral channel and camera. Diner et al. (1998) provides a detailed description of the MISR instrument. The MISR operational CTH product is derived using a stereoscopic technique, which applies feature- and area-based matching techniques between images taken from multiple cameras to measure disparities caused by cloud top height and cloud motion (Moroney et al., 2002).

Wind vectors are derived from the MISR data using a triplet set of cameras and used to correct for cloud-motion effects on the derived CTHs. The winds are derived over mesoscale domains of 70.4×70.4 km and in two altitude bins (Moroney et al., 2002). Cloud heights are reported at 1100 m spatial resolution in three wind categories. The "Best Wind" category comprises stereoscopic heights determined using the Best Quality Winds only; these were utilized exclusively for the analysis presented in Section 3.1 and in Sections 3.4–3.6 whenever possible. The "Raw Wind" category includes preliminary stereoscopic heights calculated using all available wind vectors,

regardless of their quality. These were used in Sections 3.4–3.6 if Best Wind heights were unavailable. The "No Wind" category includes stereoscopic heights calculated without a wind correction. For the scenes discussed in Sections 3.2–3.6 (for pixels producing all three height products), the average difference between Best Wind and Raw Wind CTH is about 250 m, and the average difference between Best Wind and No Wind CTH is about 500 m. The RMS error in the retrieved wind vectors is ~3 m/s, leading to uncertainties of ~300 m due to wind correction alone (Moroney et al., 2002). When combined with other sources of error, the CTH uncertainty from MISR is ~600 m (Moroney et al., 2002; Naud et al., 2004).

2.3. MODIS

The MODIS instrument has 36 spectral bands whose wavelengths range from 0.4 μm to 14.4 μm. The nominal resolution at nadir for two of the short-wave bands is 250 m; five others are at 500 m, and 29 are at 1000 m. MODIS has a ±55° scanning pattern producing a swath of 2330 km from a 705 km orbit, and achieves global coverage every one to two days (King et al., 1992). The MODIS operational cloud top pressure product (MOD06) has a horizontal resolution of 5 km. It mainly employs the CO2-slicing method (Menzel et al., 1986); however, for cloud top pressures larger than 700 hPa, the operational retrieval uses the 8, 11, and 12 μm infrared (IR) radiances, converting them to a cloud top pressure assuming an effective IR emissivity of one (Strabala et al., 1994). In our study, cloud top pressures from MODIS collection 4 are used and are then converted to heights using radiosondes from Guadeloupe. Most of the MODIS CTHs within this study were retrieved using the brightness temperature technique because trade wind cumuli typically have cloud top pressures larger than 700 mb.

3. Analysis approach and results

Our validation of trade wind cumulus CTHs addresses two separate questions: (1) how do the various retrieval algorithms perform and compare to one another, and (2) how does the spatial resolution affect the reliability of the retrievals. Both questions are addressed here through intercomparison of CTHs from four retrieval algorithms-ASTER stereo CTH and ASTER IR CTH at 90 m, MISR stereo CTH at 1100 m, and MODIS IR CTH at 5000 m spatial resolution. Note that the ASTER stereo and MISR stereo algorithms may have commonalities but are not the same, as is also the case for the ASTER IR and MODIS IR retrievals. The various sensor spatial resolutions will likely cause differences in the amount of clouds detected by each instrument (Di Girolamo & Davies, 1997). ASTER utilizes a 15 m cloud mask as described in Zhao and Di Girolamo (in press). The MISR Stereo CTH product is independent of cloud masking. The MODIS CTH algorithm uses its own radiance threshold based cloud mask product (Ackerman et al., 2002). For the purposes of this study, pixel collocation is performed prior to every comparison.

The first and most straightforward step is to compare the CTH frequency distributions from all the instruments, preserv-ing their operational or native spatial resolutions (Section 3.1). Next, the two 90 m resolution retrievals from ASTER (stereo and IR) are compared to explain the differences in performance of stereo and IR retrievals at the finest possible resolution (Section 3.2). In Section 3.3 we present how ASTER retrievals are degraded to match MISR's spatial resolution. Section 3.4 assesses the performance of two different stereo height techniques, those of ASTER and MISR. In Section 3.5, stereo (MISR) and IR (ASTER) retrievals are compared at a resolution of 1100 m. The last comparison (Section 3.6) is of stereo and IR CTHs at the coarsest resolution of 5000 m using the MISR and MODIS operational products.

It is expected that independent of the retrieval scheme (stereo or IR), cloud top heights derived from data having fine spatial resolution, such as ASTER, will produce a wider frequency distribution function enfolding the lowest and the highest cloud top heights. While for some scenes retrievals at different spatial resolutions may derive comparable mean cloud top heights, such inter-comparisons are valuable to improve the understanding and applicability of operational products which are usually available at coarser resolution.

3.1. ASTER IR, MISR stereo, and MODIS IR heights at their own spatial resolution

ASTER data were collected on 29 nonsubsequent days from September 2004 to March 2005 from 10°–20° N to 55°–65° W. This dataset is fully described in Zhao and Di Girolamo (in press). They visually inspected all ASTER scenes and excluded scenes containing any amount of cirrus and performed a statistical analysis on the remaining 157 60×60 km ASTER scenes. This yielded 1,293,959 individual clouds with a dominant effective cloud diameter of about 500 m, a peak modal cloud top height near 1 km, and an effective cloud fraction of 9% (Zhao & Di Girolamo, in press). We selected the day with the largest number of recorded scenes from each month of available data. This produced a total of 41 scenes: 11 scenes on September 17, 2004; 6 on October 29, 2004; 8 on November 28, 2004; 13 on December 9, 2004; and 3 on January 17, 2005. A comparison of the ASTER IR CTH frequency distribution from these 41 scenes against one using all 157 available cirrus-free scenes, shown on Fig. 1, finds the two maximums in Fig. 1(A) and (B) to occur at the same place-bins 750–1000 and 1250–1500. The difference between the two is that the clouds in the 750–1000 m bin is much more frequent in (A) compared to (B). Since the 41-scene dataset captures the bimodal CTH frequency distribution of the larger dataset well, the 41-scene dataset is a representative sample.

For each of the 41 scenes, we parse out data from the MISR and MODIS CTH fields that overlap with an ASTER scene and compare ASTER IR, MISR stereo, and MODIS IR (or CO_2) without degrading the resolutions to a common one; that is, ASTER IR heights are at 90 m nominal pixel size, MISR at 1100 m, and MODIS at 5000 m. The number of valid pixels derived by each algorithm is 1,411,359 (ASTER); 33,552 (MISR); and 5612 (MODIS). ASTER stereo CTHs are not included due to the heavy calculations associated with the
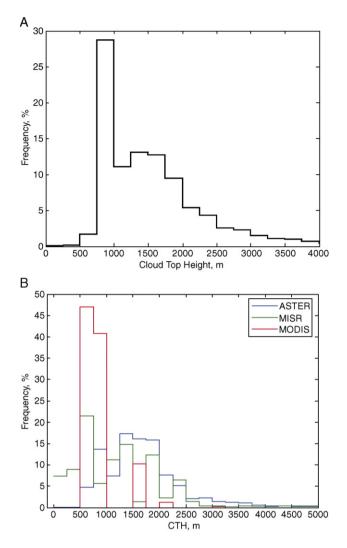
Fig. 1. Cloud top height frequency distributions: A) from ASTER at 90 m for 157 scenes; B) from ASTER at 90 m, MISR at 1100 m, and MODIS at 5000 m spatial resolution for 41 scenes.

retrieval and the large number of scenes. MISR heights are the "Best Wind" product (Section 2.2).

The histogram in Fig. 1(B) illustrates that both MISR and MODIS distributions (bin width=250 m) substantiate the bimodal distribution observed with ASTER. The first distinct maximum detected by ASTER is at 750–1000 m and is located at 500–750 m by MISR and between 500 and 1000 m by MODIS. MISR, alone of the three instruments, also places a substantial population in the 0–500 m bins. The second maximum is wider: three ASTER bins of similar CTH frequency between 1250 and 2000 m enclose two MISR peaks at 1250–1500 m and 1750–2000 m, while MODIS exhibits its secondary maximum at 1500–1700 m, but with a much lower frequency. In contrast to the other two instruments, MODIS detected few CTHs above 1750 m. Thus, while all three instruments capture a bimodality in CTH that appears to be basic to these trade wind cumulus fields, the differences between the products are noteworthy.

To gain an understanding on the causes behind the differences in CTH statistics between the three instruments, several scenes were examined in detail. Sections 3.2–3.6 present the results of a thorough investigation of one of these scenes, the "showcase" scene, that encapsulates the findings of all scenes. An ASTER image of the showcase scene is shown in Fig. 2.

3.2. ASTER stereo and ASTER infrared (IR) heights at 90 m resolution

The coexistence of stereo and IR retrievals from ASTER at a spatial resolution of 90 m is valuable for avoiding the collocation and coregistration issues associated with multi-instrument data fusion. Fig. 3A shows the ASTER stereo (top left) and IR height fields (top middle), as well as the difference between them (top right). On the bottom row of Fig. 3A are the CTH distributions for each top-row image; the *x*-axis is the frequency as a percentage value, and the *y*-axis is the CTHs in meters. Table 1 provides a statistical summary from the analysis of this scene.

Fig. 3B is similar to Fig. 3A but is limited to those pixels where CTH was retrieved by both methods. A careful visual comparison of the images from Fig. 3A and B reveals the location of the pixels "missed" by each of the retrievals. The pixels present in the stereo CTH of Fig. 3A but missing in Fig. 3B are mostly very small clouds falling in the 500–750 m altitude bin (compare also the respective histograms). Since the stereo CTH of Fig. 3B contains only those stereo-retrieved heights for which IR retrievals are also available, this implies that low-lying fully cloud-covered pixels at 90 m resolution remain a problem for IR retrieval. Such clouds still possess a significant visual contrast from the surface, reflective of the liquid phase, and are less problematic for stereo retrieval. Another area of discrepancy between the two retrievals occurs with the higher, thin diffuse cloud to the center right of the cloud in Figs. 2 and 3A. Here the contrast may seem low to the human eye (see Fig. 2), while at the same time the thermal contrast is more pronounced (not shown). Nevertheless the stereo approach successfully retrieves a CTH for a larger cloud portion than does the IR. This suggests that the low visual contrast is not as problematic for stereo retrieval as the low emissivity may be for IR retrieval.
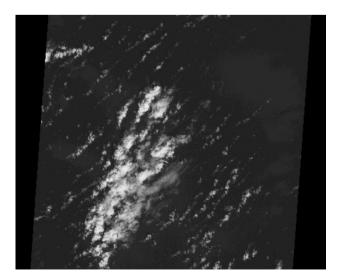

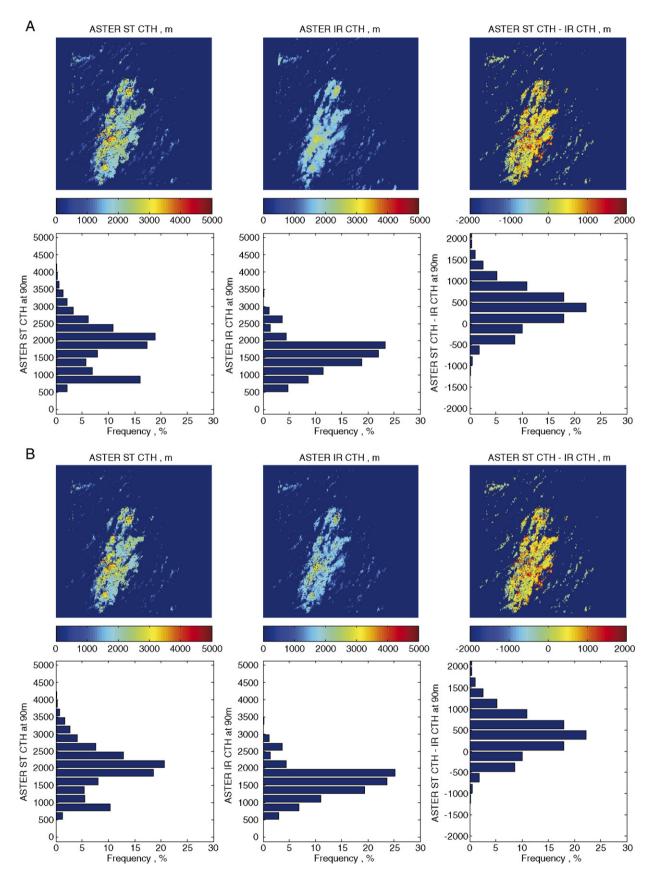Fig. 2. ASTER *show case* scene, December 9, 2004, 14:42:57 Z.

Fig. 3. ASTER Stereo and Infrared CTH comparison at 90 m spatial resolution— A) all pixels; (B) only pixels retrieved by both retrievals. Plots are arranged from left to right as follows: ASTER stereo CTH, ASTER IR CTH, and CTH differences; underneath are the corresponding histograms.

Table 1
ASTER cloud top heights — statistical summary for the "show case"

Show case	ASTER STEREO CTH, m	ASTER IR CTH, m
Number of pixels	79291	74618
Min	738	528
Max	5356	3664
Mean	1676	1420
Median	1849	1546
Standard	211	123

Another difference between the stereo and IR approaches is seen in the central part of the cloud, where the stereo-derived heights exceed the IR CTHs. Since the optical depth in the center of the cloud is probably higher than at the edges, we believe that the IR emissivity assumption of 1.0 is correct. The issue here may be the influence of cloud morphology on stereo retrieval: the cloud is bright, with its geometry interacting significantly with the incoming solar radiation, and may be developing rapidly as evidenced by the presence of turrets in Fig. 2. This suggests that the use of contrast in the short-wave channels to match cloudy pixel pairs may be more prone to erroneous height retrievals for this portion of the cloud.

When both retrievals derive a CTH, the stereo retrieval places the CTH higher than IR retrieval (Fig. 3B, top left and middle panels). As seen in the stereo-IR CTH difference plots and histograms, the height difference occurs regardless of pixel-scale cloud height, horizontal size, or IR opacity. The mean difference is about 250 m. One likely explanation is bias introduced into the stereo CTH through the use of GOES cloud-tracked winds. It is also possible that the vertical weighting functions for where most of the reflected vs. emitted photons are originating are slightly different.

Lastly, we note that both retrievals produce CTHs for approximately 20% of the cases missed by the other retrieval, suggesting that a combined IR-stereo CTH retrieval could be fruitful if laborious. The pixels captured by the IR algorithm but missed by the stereo algorithm are usually evenly distributed throughout the entire image and at all height bins. This reflects the increased complexity of the stereo retrieval compared to the IR retrieval.

3.3. Degrading ASTER resolution

We sought to explore the sensitivity of the stereo and IR retrievals to spatial resolution by degrading the ASTER data from 90 m to the 1100 m spatial resolution characterizing the MISR CTH retrievals. As a first step we degraded the ASTER stereo and IR CTHs rather than the ASTER radiances. For simplicity the pixels are assumed to have a circular shape, so that on average it takes about 150 90 m pixels to "form" one 1100 m pixel. The representative CTH for each 1100 m pixel could then be either the mean or the median of the available CTHs from the cloudy 90 m pixels. Fig. 4 illustrates the difference between the means and medians for both the IR and stereo retrievals as a function of the number of cloudy 90 m pixels contributing to one 1100 m pixel, with the red curve providing the best fit to the data (Fig. 4A and B, respectively). Both retrievals show a wide range of differences between the mean and median values. However, the

stereo (mean–median) CTH difference is not sensitive to cloud fraction, while the IR (mean–median) CTH difference does depend on cloud fraction. The ASTER stereo approach appears more appropriate at low cloud fractions and that it is not sensitive to the choice of the mean or median statistic. Nevertheless, we selected the median as our statistic of choice because it is less influenced by outlying values than the mean. Next, the ASTER stereoscopic retrieval is applied to the showcase scene radiances, after they have been degraded to 1100 m spatial resolution simply by averaging the original 15 m radiances.

3.4. ASTER stereo and MISR stereo heights at 1100 m resolution

In Fig. 5 we intercompare ASTER and MISR stereo heights at 1100 m for the "showcase" scene, where the ASTER stereo retrieval is degraded to match MISR spatial resolution. The wind correction for the ASTER heights (derived using the GOES winds) is 738 m. The MISR wind correction is 750 m. As the two are very close, we believe that the comparison can provide insight into the two algorithms independent of cloud-motion effects and also into the impact of spatial resolution. The
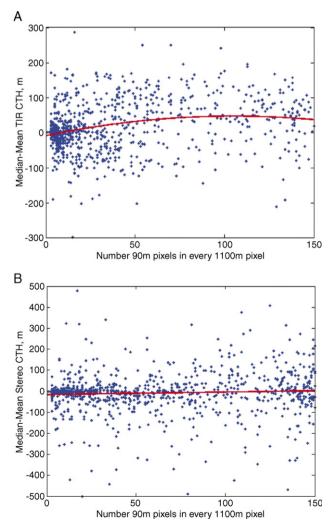

Fig. 4. Differences between ASTER median and mean of the 90 m spatial resolution pixels forming each 1100 m pixel: A) infrared retrieval; B) stereo retrieval.
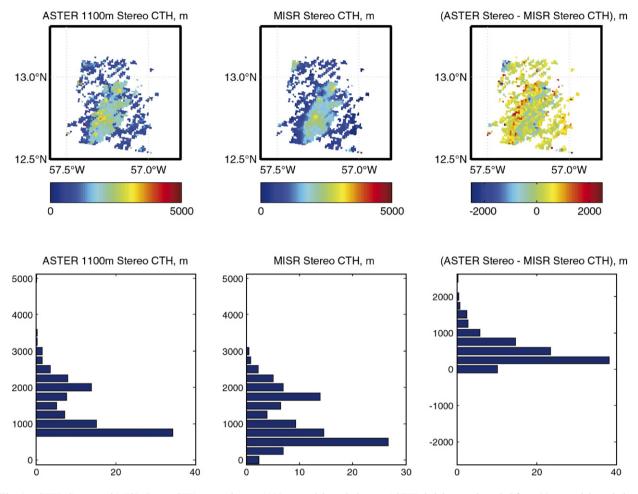
Fig. 5. ASTER Stereo and MISR Stereo CTH comparison at 1100 m spatial resolution — ASTER heights are degraded from 90 m spatial resolution.

other two analyzed scenes revealed that wind correction could make as much as a 300 m difference in the final CTH product. The averaged wind speed for all three scenes is 10.5 m/s. The ASTER 1100 CTH field is constructed in a way (see Section 3.3) that should imply similar values to the higher-resolution 90 m CTH field. It is therefore of interest that the CTH histograms of the two are not entirely similar (Figs. 3B and 5, lower left panels). Although the two CTH frequency maxima occur at the same heights, when the resolution is degraded to 1100 m the relative frequency of the lower maximum is increased at the expense of the higher-altitude frequency maximum. The reduced number of higher-altitude values within the 1100 m CTH distribution demonstrates that many of the higher CTH values occur on spatial scales that are less than 1100 m. It is unclear whether these high values are high-spatial-frequency-noise in the retrieval or actual small-scale features or a combination of both. Discrimination between these two explanations requires more data and further analysis.

The ASTER and MISR CTH fields are shown in the top two left panels of Fig. 5; underneath are the corresponding histograms. Occasional very high stereo heights caused by blunders have been filtered out. Both methods derive a bimodal distribution, but the lower ASTER maximum is 250 m (one bin) higher than the MISR lower maximum (750–1000 m vs. 500–750 m). The ASTER CTH distribution shows no clouds with

CTH less than 750 m. Fig. 6 shows a height distribution of ceilometer-derived cloud base heights taken during January 9–23 from the RICO Research Vessel Seward Johnson; this shows that few cloud bases existed below 600 m, with the highest frequency occurring at 1100–1200 m. RICO research flight observations also indicated that a typical trade wind cumulus cloud base height is about 500–600 m. As reported by Naud et al. (2005), MISR CTHs lower than 562 m (the uncertainty of MISR CTH) are unreliable and should be excluded from further analysis; this finding is supported further here.

The panels on the right-hand side (both rows) of Fig. 5 show that ASTER CTHs are on average higher than MISR CTHs by 450 m. While some of the difference could reflect cloud motion error, the higher-mean-altitude ASTER CTHs are also more consistent with the ceilometer-derived cloud base height frequency maximum at 1000–1100 m than the MISR CTHs. One explanation for the difference between the ASTER and MISR CTHs might be the higher initial spatial resolution of the ASTER data, allowing for a more thorough and sensitive initial matching.

Fig. 7 presents the comparison of ASTER stereo heights derived from degraded radiances against the MISR stereo CTH. The first observation is that many small clouds have been undetected because their effective size is smaller than 1100 m. This confirms cloud detection and CTH retrieval are linked. The ASTER stereo heights histogram is no longer bimodal. The
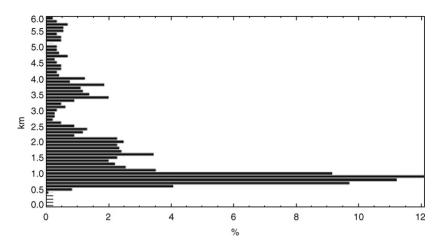
Fig. 6. Surface-based vertically-pointing ceilometer-derived cloud base height frequency distribution spanning Jan. 9–23, 2004, taken from the Research Vessel Seward Johnson as part of the RICO field campaign. Cloud base heights represent median values duirng a 10-min time interval. The ceilometer has a height accuracy of approximately 30 m.

MISR height distribution preserves the bimodality however — the area matching and displacement determination within the MISR retrieval is performed for single 275 m pixel. Hence a match is more probable to be representative of a small and not quite developed cloud with lower CTH. The mean height difference for this comparison is 580 m.

3.5. ASTER infrared and MISR stereo heights at 1100 m resolution

Fig. 8 shows the ASTER IR and MISR stereo CTH fields at spatial resolution of 1100 m and their differences. The lower frequency maximum in the 1100 m ASTER IR CTHs is similar
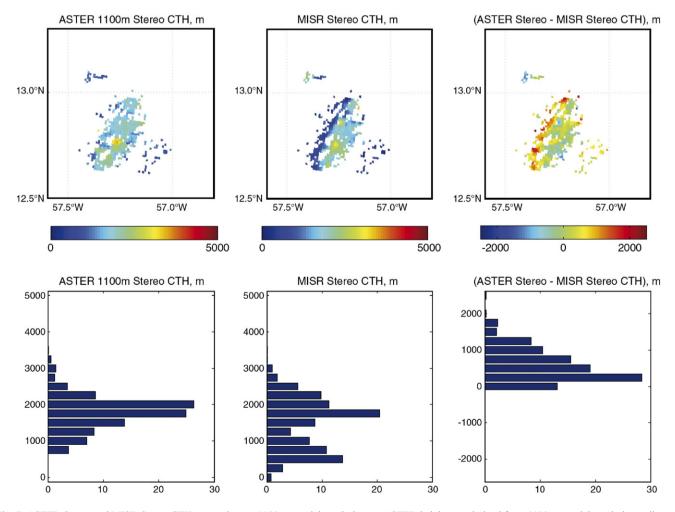

Fig. 7. ASTER Stereo and MISR Stereo CTH comparison at 1100 m spatial resolution — ASTER heights are derived from 1100 m spatial resolution radiances.

to that for the stereo CTHs, but the frequency maximum at 2000–2250 m that is present in the stereo CTHs appears to be displaced to a lower altitude in the IR CTHs. The ASTER IR 1100 m CTH distribution is also quite different from the IR CTH distribution at 90 m. Nearly 40% of the clouds at 1100 m resolution have CTHs between 750 and 1000 m, and only about 12% of the pixels have CTHs between 1750 and 2000, while at 90 m, 7% of the pixels fall into the 750–1000 m bin and 25% fall into the 1750–2000 bin. Apparently the IR CTH algorithm is strongly sensitive to data spatial resolution. It appears to be least accurate in areas with a lot of cloud height variability, as evidenced by the central part of the cloud, where both stereo retrievals and the IR 90 m retrieval show more high cloud tops than does the IR 1100 m retrieval. This portion of the cloud consists of rapidly developing turrets (Fig. 2).

3.6. MISR stereo and MODIS infrared heights at 5000 m resolution

Comparison of the MISR stereo CTHs to the various ASTER retrievals shows that although the MISR retrievals appear to have a low bias of approximately 250 m locating the maxima and include many erroneously low CTH values, the MISR stereo retrieval captures the bimodality and the relative fre-

quencies of the lower or higher clouds approximately correctly. Our last comparison is of the MISR stereo and MODIS IR CTHs, both at a spatial resolution of 5000 m. It is shown on Fig. 9. Only the MISR CTHs for the 1100 m "cloudy" pixels were averaged. The mean difference between MISR and MODIS heights is −495 m; the distributions clearly indicate a negative bias for the MODIS heights. Almost half of the MODIS heights appear to be below 500 m, which is inconsistent with the ceilometer-derived cloud base heights (Fig. 6). For this comparison we used MODIS collection 4 cloud products; the CTH retrieval algorithm averages the radiances from 5×5 1 km pixels to calculate one radiance and a CTH for it, and the clear pixels will negatively bias the MODIS CTHs. In the next MODIS collection, only cloudy pixels will be used and the MODIS CTHs should be improved.

Preliminary statistics derived over the tropics and using 5 km spatial resolution IR CTPs report 39.7% low clouds (Zhang Hong, personal communications, June 2006). The amount of low clouds is reduced to 30.1% if the 1 km IR CTH are used. Retrievals at both spatial resolutions used the same cloud mask, hence the same cloud populations have been targeted. This leads us to believe the difference in amount of low clouds is due to spatial resolution effects, i.e. the heights at 5 km are underestimated and thus yield faultily more low clouds. This
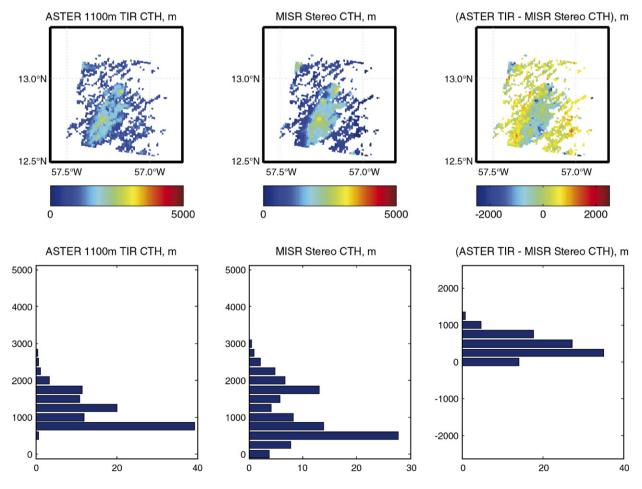

Fig. 8. ASTER Infrared and MISR Stereo CTH comparison at 1100 m spatial resolution.
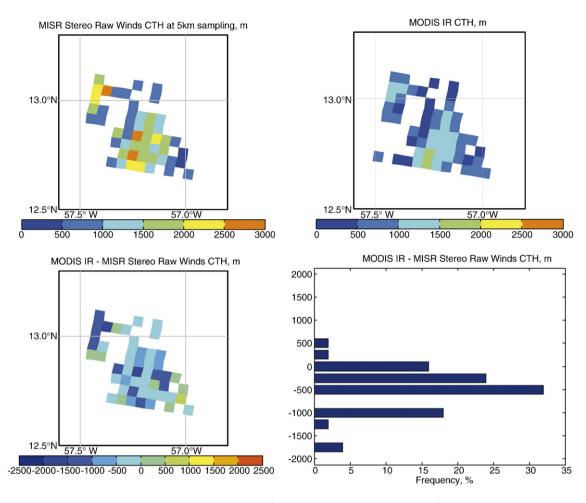
Fig. 9. MISR Stereo and MODIS Infrared CTH comparison at 5000 m resolution.

conclusion is in agreement with previous studies of MODIS heights (Naud et al., 2005) which have found MODIS CTH to have a low bias in comparison with MISR CTH.

4. Summary and conclusions

The Terra products presented here are part of an effort to understand the uncertainties of satellite-derived CTHs. Data from 3 satellite instruments are examined, with CTHs retrieved using 2 different techniques. The resolutions examined span from smaller to larger than the average effective size of trade wind cumuli. The analysis of 41 60×60 km scenes shows that ASTER, MISR, and MODIS retrievals all exhibit a bimodal CTH distribution also observed in higher-vertical-resolution ceilometer-derived cloud base heights, independent of retrieval approach and spatial resolution, but with significant differences between the distributions. Several individual scenes were more thoroughly studied and Table 2 summarizes the cloud top height mean differences for a "showcase" scene (Section 3.1).

The ASTER stereo height retrieval at 90 m produced the highest mean CTHs, exceeding those of the ASTER IR retrieval by 250 m mean bias. A likely explanation of the difference in mean height is cloud motion that is unaccounted for by the ASTER stereo retrieval, which relies on cloud motion winds from an ancillary source. At the lower spatial resolution of

1100 m, ASTER stereo and IR heights exceeded MISR stereo CTHs by 450 m and 415 m mean bias, respectively. The ASTER data degradation was performed on the 90 m ASTER CTHs first, and then on the 15 m radiances. The ASTER stereo height from degraded radiances loses bimodality and reports 580 m mean cloud top height difference from MISR for the showcase scene. The MISR CTH retrieval captured the relative frequency of the bimodal approximately correctly but located the maxima approximately 250 m lower than ASTER. MISR CTH also has a much higher uncertainty of 500 m that may explain the high frequency of erroneously low values. Despite the low bias, the MISR CTHs were still higher than the MODIS IR-derived heights by 580 m at a spatial resolution of 5000 m. A probable cause of this difference is the occasional inclusion of

Table 2
ASTER, MISR and MODIS cloud top height mean differences for the "show case"

Retrieval method	Resolution, m	Mean CTH Difference, m
ASTER stereo — ASTER IR	90	250
ASTER stereo — MISR stereo	1100	450
ASTER stereo — MISR stereo (degraded radiances)	1100	580
ASTER IR — MISR stereo	1100	415
MISR stereo — MODIS IR	5000	580

clear 1000 m pixels within the 5000 m pixels the MODIS algorithm is applied to, a calculation that will be discontinued for the next MODIS collection.

A comparison to ceilometer-derived cloud base heights suggests the ASTER stereo retrievals are probably the most accurate. The biases we have discussed imply that ASTER stereo CTHs should be expected to be higher than MODIS CTHs by 1050 m in the mean. Independent video CTHs derived with an airborne camera during RICO show similar differences between MODIS and video heights—the video heights vary between 850 m and 1700 m, and depend on the time interval between the aircraft flight and the satellite overpass of between 2 and 5 min (Genkova et al., 2005).

Bimodality in CTHs appears to be a central feature of trade wind cumulus clouds and even occurs within the same cloud. The physics requires further study, suggesting either variability in the trade wind capping inversion, or the prevalence of "chimney" clouds, where the most actively-convecting cloudy parcel is able to penetrate above the inversion. One result of our study is that most satellite-derived CTHs are able to resolve this trade-wind Cu bimodality, and therefore may be able to help in its interpretation. Although both ASTER retrievals capture the bimodality the best of the 3 satellite instruments, these retrievals are not regularly available. MISR stereo-derived CTHs are an easily available operational product and also capture the CTH bimodality. Infrared-derived CTHs, however, are by far the most widely used, and MODIS has the advantage over MISR of far greater spatial coverage (the MODIS instrument is present on two satellite platforms, and each swath is approximately six times the width of a MISR swath). Since stereo retrievals are currently applicable only to ASTER and MISR data, IR-derived CTHs will remain important. The IR-derived CTHs evaluated within this study are more affected by spatial resolution than stereo-retrieved CTHs, with the ASTER IR distribution showing significantly lowered CTHs upon spatial degradation as well as an altered distribution, even though only the CTHs themselves were degraded and not the radiances. One result from this study therefore is a recommendation that IR-derived CTHs be produced at the highest spatial resolution possible, with subsampling preferred over spatial averaging. Since many cumulus clouds have horizontal dimensions less than 1 km, a good, widely available IR-derived CTH product will remain a challenge. The current MODIS operational CTH product, besides providing unrealistically low CTHs, also does not appear to capture the inherent CTH bimodality and will need to be reevaluated for trade wind cumulus studies after the next collection becomes available.

Ackowledgements

References

Ackerman, S., Strabala, K., Menzel, P., Frey, R., Gumley, L., Baum, B., et al. (2002). *Discriminating clear-sky from cloud with MODIS — Algorithm theoretical basis document.* Products: MOD35. ATBD reference number: ATBD-MOD-06.

Alley, R., & Jentoft-Nilsen, M. (2001). *Algorithm theoretical basis document for brightness temperature.*: Jet Propulsion Laboratory http://eospso.gsfc. nasa.gov/eos_homepage/ for_scientists/atbd/docs/ASTER/BTS_ATBD.pdf

Benner, T. C., & Curry, J. A. (1998). Characteristics of small tropical cumulus clouds and their impact on the environment. *Journal of Geophysical Research, 103,* 28753−28768.

Bony, S., & Dufresne, J. -L. (2005). Marine boundary layer clouds at the heart of cloud feedback uncertainties in climate models. *Journal of Geophysical Research, 32,* L20806. doi:10.1029/2005GL023851

Di Girolamo, L., & Davies, R. (1997). Cloud fraction errors caused by finite resolution measurements. *Journal of Geophysical Research, 102,* 1739−1756.

Diner, D. J., Beckert, J. C., Reilly, T. H., Bruegge, C. J., Conel, J. E., Kahn, R. A., et al. (1998). Multi-angle Imaging SpectroRadiometer (MISR) instrument description and experiment overview. *IEEE Transactions on Geoscience and Remote Sensing, 36,* 1072−1087.

Genkova, I., Zhao, G., Seiz, G., Snodgrass, E., Colon, M., Di Girolamo, L., & Rauber, R. (2005). Validation of trade wind cumulus cloud properties produced by meteorological satellites. *Proceedings of SPIE, Remote Sensing of Clouds and the Atmosphere X, Vol. 5979,* 0-8194-5999-2 Pub. Oct 2005; Softcover; In Print.

King, M. D., Kaufman, Y. J., Menzel, W. P., & Tanre, D. (1992). Remote sensing of cloud, aerosol, and water vapor properties from the Moderate Resolution Imaging Spectrometer (MODIS). *IEEE Transactions on Geoscience and Remote Sensing, 30,* 2−27.

McFarquhar, G. M., Platnick, S., Di Girolamo, L., Wang, H., Wind, G., & Zhao, G. (2004). Trade wind cumuli statistics in clean and polluted air over the Indian Ocean from in situ and remote sensing measurements. *Geophysical Research Letters, 31,* l21105. doi:10.1029/2004gl020412

Menzel, W. P., Wylie, D. P., & Huang, A. H. -L. (1986). Cloud top pressures and amounts using HIRS CO_2 channel radiances. *Technical proceedings of the third international TOVS study conference, 13–19 August 1986, Madison, WI* (pp. 173−185).

Moroney, C., Davies, R., & Muller, J. -P. (2002). Operational retrieval of cloud top heights using MISR data. *IEEE Transactions on Geoscience and Remote Sensing, 40,* 1532−1540.

Naud, C. M., Muller, J. -P., Clothiaux, E. E., Baum, B. A., & Menzel, W. P. (2005). Intercomparison of multiple years of MODIS, MISR and radar cloud-top heights. *Annals of Geophysics, 23,* 2415−2424.

Naud, C., Muller, J., Haeffelin, M., Morille, Y., & Delaval, A. (2004). Assessment of MISR and MODIS cloud top heights through inter-comparison with a back-scattering lidar at SIRTA. *Geophysical Research Letters, 31,* L04114. doi:10.1029/2003GL018976

Rangno, A. L., & Hobbs, P. V. (2005). Microstructures and precipitation development in cumulus and small cumulonimbus clouds over the warm pool of the tropical Pacific Ocean. *Quarterly Journal of the Royal Meteorological Society, 131,* 639−673.

Rossow, W. B., & Garder, L. C. (1993). Cloud detection using satellite measurements of infrared and visible radiances for ISCCP. *Journal of Climate, 6,* 2341−2369.

Seiz, G., Baltsavias, E., & Gruen, A. (2002). 3D-Wolkenmodellierung für Wetter-und Klimamodelle, Vermessung. *Photogrammetrie und Kulturtechnik, 10,* 626−629.

Seiz, G., Davies, R., & Gruen, A. (2006). Stereo cloud-top height retrieval with ASTER and MISR. *International Journal of Remote Sensing, 27*(9) (May 10), 1839−1853.

Short, David A., & Nakamura, Kenji (2000). TRMM radar observations of shallow precipitation over the tropical oceans. *Journal of Climate, 13*(23), 4107−4124.

Strabala, K. I., Ackerman, S. A., & Menzel, W. P. (1994). Cloud properties inferred from 8–12 micron data. *Journal of Applied Meteorology, 33,* 212−229.

Velden, C. S., Daniels, J., Stettner, D., Santek, D., Key, J., Dunion, J., et al. (2005). Recent innovations in deriving tropospheric winds from

meteorological satellites. *Bulletin of the American Meteorological Society*, *86*, 205−223.

Warren, S. G., Hahn, C. J., London, J., Chervin, R. M., & Jenne, R. (1986). *Global distribution of total cloud cover and cloud type amounts over land, DOE/ER/60085-H1, NCAR Tech. Note TN-273 +STR.* Boulder, Colorado: National Center for Atmospheric Research 231 pp.

Xue, H., & Feingold, G. (2006). Large eddy simulations of trade wind cumuli: Investigation of aerosol indirect effects. *Journal of the Atmospheric Sciences*, *63*(6), 1605−1622.

Yamaguchi, Y., Kahle, A. B., Tsu, H., Kawakami, T., & Pniel, M. (1998). Overview of advanced spaceborne thermal emission and reflection radiometer, ASTER. *IEEE Transactions on Geoscience and Remote Sensing*, *36*, 1062−1071.

Zhao, G., & Di Girolamo, L. (in press). Statistics on the Macrophysical Properties of Trade Wind Cumuli over the tropical western Atlantic. *Journal of Geophysical Research*.